# CrystEngComm

Accepted Manuscript






ROYAL SOCIETY OF CHEMISTRY

www.rsc.org/crystengcomm

Journal Name

RSCPublishing

ARTICLE

# New lanthanide coordination frameworks constructed from 1,3- benzenedicarboxylate-oxalate mixed linkers and terminal 1,10-phenanthroline: Crystal structure, multicolor luminescence and high-efficiency white light emission

Cite this: DOI: 10.1039/x0xx00000x

Received 00th January 2012,
Accepted 00th January 2012

DOI: 10.1039/x0xx00000x

www.rsc.org/

Rui Huo, Xia Li,* and Dou Ma

New complexes, $[Ln_2(1,3\text{-}BDC)_2(phen)_2(ox)(H_2O)]$ (Ln = Eu **1**, Tb **2**, and Yb **3**, 1,3- BDC – 1,3- benzenedicarboxylate, ox = oxalate, and phen = 1,10-phenanthroline), have been obtained under hydrothermal condition. The isostructural complexes **1- 3** have 3D structures with helical chains assembled from tetrameric secondary building units (SBUs) by 1,3-BDC and ox- mixed linkers. Complex **1** shows a red luminescence with a high quantum yield (Φ= 63.21%) of Eu(III) ($^5D_4 \rightarrow {}^7F_{0\text{-}4}$), while complex **2** exhibits a green luminescence (Φ= 10.13%) of Tb(III) ($^5D_4 \rightarrow {}^7F_{6\text{-}2}$). The Yb,Tb,Eu doped complex reveals a significant multicolor luminescence from blue, green, yellow to white regions, through the tuning of the excitation wavelengths. A high-efficiency white light emission (Φ=20.4%) was achieved. Energy transfer from Tb(III) to Eu(III) has been observed.

## 1. Introduction

Metal–organic frameworks (MOFs) have been intensively studied during the past few years because of their interesting architectures and potential applications in the areas of gas storage, catalysis, separation, magnetism, and optics.[1] Much of this attention was particularly focused on the crystal engineering dealing with the design and synthesis of MOFs for their novel structures, properties and potential applications. Lanthanide- -based organic frameworks (LnOFs) have received considerable attention due to their interesting photophysical properties, such as intense emission, narrow bandwidth, and long lifetime, ranging from the UV to the NIR spectral regions.[2] These materials have many potential applications in a variety of areas such as energy-harvesting devices, optical displays, and luminescent probes, etc.[3] It is noteworthy that Ln(III) doped materials can produce tunable luminescence via the combination of different color emissions from Ln(III) center. With judiciously chosen red-, green-, and blue-emissive ions doped in a suitable host, it is possible to obtain phosphors which emit across the entire visible spectrum, including white light. This has potential applications in multicolor displays and light-emitting diodes (LEDs).[4] Although the tunable white light emission of LnOFs has been recently investigated,[5] many of those reported emissions have low quantum yields.[5e-i] When the Ln(III) ion coordinates with a ligand, efficient energy transfer from the ligand to Ln(III) ion is facilitated. The low absorption coefficients of Ln(III) ions significantly increase with the strong absorbance of organic ligands, leading to the intense luminescence of Ln(III) ions.[2] Furthermore, due to the richness of organic ligands, the association of metal centers with organic linkers gives rise to a wide variety of arrangements. Thus, to reach LnOFs, it is essential to design and synthesize LnOFs with novel molecular architectures and appealing photophysical properties, such as intense photoluminescence, for luminescent applications.

Here, we are reporting some of our current work exploring novel luminescent MOFs and tunable luminescence of the doped Ln(III) system. Our design focuses on obtaining high-efficiency luminescent LnOFs. As is known, the versatility of the 1,3-benzenedicarboxylate (1,3-BDC) ligand is demonstrated by the structures described in the literature.[6,7] 1,10-phenanthroline (Phen) is the best ancillary antenna ligand for luminescent complexes. Therefore, $[Ln_2(1,3\text{-}BDC)_2(phen)_2(ox)(H_2O)]$ (Ln = Eu **1**, Tb **2**, Yb **3,** ox = oxalate) complexes were prepared. This system featured the combination of 1,3-BDC - ox mixed linkers and phen ancillary ligand. The resulting complexes showed novel 3D frameworks different from the Ln(III) complexes containing1,3-BDC in the literature.[7] Tb(III) complex (**2**), particularly Eu(III) complex (**1**) showed high luminescence quantum yields. The tunable multicolor emission of a doping of lanthanide framework (Yb:Tb:Eu) was also investigated, and it was proposed that Tb(III) could assist sensitization of Eu(III). It is noteworthy that white light emission had high quantum yield of 20%.

## 2. Experimental section

### 2.1 Materials and physical measurements

$Ln(NO_3)_3{\cdot}6H_2O$ (Ln = Eu, Tb and Yb) were prepared by the corresponding oxide with nitric acid. Other reagents were

commercially available and were used without further purification.

The elemental analyses (C/H/N) were obtained on a Vario EL elemental analyzer. Infrared (IR) spectra were measured on a Bruker Tensor37 spectrophotometer using the KBr pellets technique. Experimental powder X-ray diffraction (PXRD) was carried out on a PANaytical X' Pert PRO MPD diffractometer with $CuK_\alpha$ radiation ($\lambda$ = 1.5406 Å), with a scan speed of $2°\cdot min^{-1}$ and a step size of 0.02° in 2θ. The simulated PXRD patterns were obtained from the single-crystal X-ray diffraction data. Thermogravimetric analyses (TGA) were carried out using a HCT-2 thermal analyzer under air from room temperature to 800 °C with a heating rate of 10 °C/min. Solid state excitation and emission spectra were recorded on an FL4500 fluorescence spectrophotometer (Japan Hitachi company) at room temperature. The fluorescence lifetimes were measured on FLS920 Steady State &Time-resolved Fluorescence Spectrometer (Edinburgh Instrument). The emission quantum yields were measured using a Quantum Yield Measurement System Fluorolog®-3 (HORIBA company) with a 450W Xe lamp coupled to a monochromator for wavelength discrimination, an integrating sphere as sample chamber, and an analyzer R928P for signal detection. The CIE (Commission International de I'Eclairage) color coordinates were calculated on the basis of the international CIE standards.[8]

### 2.2 Synthesis of complexes

A mixture of $Ln(NO_3)_3\cdot 6H_2O$ (0.1 mmol) (Ln = Eu **1,** Tb **2** and Yb **3**), 1,3- benzenedicarboxylate (0.2 mmol), oxalate (0.1 mmol), 1,10-phenanthroline (0.2 mmol), 10 mL $H_2O$ and an aqueous solution of NaOH (2 mol/L, 0.20 mL) was sealed in a 25 mL Teflon-lined stainless steel autoclave. The mixture was heated at 140 ºC for 3 days. The synthetic scheme is listed in Scheme S1a. Yield: 60% for **1**, 66% for **2**, and 65% for **3** based on the Ln(III). For **1**: Anal. Calc. for $C_{42}H_{26}N_4O_{13}Eu_2$: C, 45.92; N, 5.10; H, 2.38%.Found: C, 45.88; N, 5.01; H, 2.67%. Selected IR (KBr pellet, $cm^{-1}$): 3429(vs) 、 1672(vs) 、 1610(vs) 、 1575(s) 、 1554(s) 、 1519(m) 、 1478(w) 、 1449(m) 、 1392(vs) 、 1313(m) 、 1165(w) 、 1103(w) 、 937(w) 、 864(w) 、 848(w) 、 828(w) 、 790(w) 、 745(m) 、 730(w)、713(w)、690(w)、639(w)、524(w)、419(w). For **2**: Anal. Calc. for $C_{42}H_{26}N_4O_{13}Tb_2$: C, 45.34; N, 5.04; H, 2.36%.Found: C, 45.46; N, 4.96; H, 2.76%. Selected IR (KBr pellet, $cm^{-1}$): 3424(vs) 、 1674(vs) 、 1610(vs) 、 1577(s) 、 1553(s) 、 1519(m) 、 1479(w) 、 1450(m) 、 1392(vs) 、 1314(m)、1158(w)、1104(w)、938(w)、864(w)、848(w)、830(w) 、 792(w) 、 745(m) 、 729(w) 、 714(w) 、 691(w) 、 639(w) 、 525(w) 、 420(w). For **3**: Anal. Calc. for $C_{42}H_{26}N_4O_{13}Yb_2$: C, 44.82; N, 4.91; H, 2.30%.Found: C, 45.05; N, 4.79; H, 2.53%. Selected IR (KBr pellet, $cm^{-1}$): 3428(vs) 、 1674(vs) 、 1612(vs) 、 1577(s) 、 1555(s) 、 1520(m) 、 1479(w) 、 1451(m) 、 1394(vs) 、 1315(m) 、 1167(w)、1104(w)、940(w)、865(w)、848(w)、830(w)、792(w) 、 745(m) 、 732(w) 、 715(w) 、 693(w) 、 640(w) 、 524(w)、420(w).

For Yb,Tb,Eu-doped coordination network, the synthetic method is same as mentioned above just by loading the corresponding $Ln(NO_3)_3\cdot 6H_2O$ as the starting materials in stoichiometric ratios. For $Yb_{0.73}Tb_{0.25}Eu_{0.02}$ doped complex. Selected IR (KBr pellet, $cm^{-1}$): 3430(vs) 、 1674(vs) 、 1608(vs) 、 1576(s) 、 1555(s) 、 1519(m) 、 1479(w) 、 1450(m) 、 1394(vs) 、 1313(m) 、 1166(w) 、 1101(w) 、 938(w) 、 865(w) 、 848(w) 、 826(w) 、 791(w) 、 746(m) 、 731(w)、715(w)、692(w)、640(w)、525(w)、419(w).

### 2.3 X-ray Crystallography Study

The X-ray single crystal data collections for the three complexes were performed on a Bruker Smart Apex II CCD diffractometer equipped with a graphite monochromated Mo Kα radiation ($\lambda$ = 0.71073 Å) at 293(2) K. Semiempirical absorption correction was applied using the SADABS program.[9] The structures were solved by direct methods and refined by full matrix least squares method on $F^2$ using SHELXS 97 and SHELXL 97 programs.[10] The selected bond lengths of complexes **1**–**3** are listed in Tables S1.

## 3. Results and discussion

### 3.1 Crystal structures

The complexes $[Ln_2(1,3\text{-}BDC)_2(phen)_2ox\cdot H_2O]$ (Ln = Eu **1,** Tb **2,** and Yb **3**) crystallize in a triclinic system, Pī space group, and are isostructural (Fig. S1). Within these compounds, the corresponding distances of Ln-O, Ln-N, and Ln…Ln (Table S1) decrease due to the decrease of ion radii from Eu(III) to Yb(III) ion. Herein only structure **1** will be discussed in detail. The asymmetric unit of **1** contains two Eu(III) ions, two 1,3-BDC, two phen, one ox, and one water molecule. It is interesting to note that there are two types of Eu(III) ion environments, Eu1 and Eu2 (Fig. 1a). Eu1 ion is eight- coordinated by four oxygen atoms from three 1,3-BDC ligands, two oxygen atoms from an ox group, and two nitrogen atoms from a phen ligand. Eu2 ion is eight- coordinated by three oxygen atoms from two1,3-BDC ligands, two oxygen atoms from an ox group, one oxygen atom from a water molecule, and two nitrogen atoms from phen ligand. The Eu−O distances to the carboxylate, ox, and water groups are in the range of 2.278(6) - 2.439(7), 2.390(6) - 2.458(6), and 2.325(7) - 2.489(7) Å, respectively. The Eu–N bond lengths range from 2.575(8) to 2.631(8) Å. The 1,3-BDC ligands adopt two coordination modes, $\mu_2$:$\eta^1\eta^1$/$\mu_1$:$\eta^1$ and $\mu_1$:$\eta^1\eta^1$/$\mu_2$:$\eta^1\eta^1$ (Scheme S1b). The carboxylate groups of 1, 3-BDC are twisted relative to their respective aromatic ring planes by 8.2°/15.9° and 16.1°/164.3°. Ox adopts $\mu_2$:$\eta^1\eta^1$/$\mu_2$:$\eta^1\eta^1$ coordination mode and links two different Eu(III) ions. Eu1 and Eu2 ions are connected by one ox group to form a [Eu1-ox-Eu2] dimeric unit. The [Eu1-ox-Eu2] units containing Eu1 and Eu2 ions are linked together by double 1, 3-BDC ligands to form centrosymmetric tetradmeric units [Eu1-ox-Eu2]-1,4BDC-[Eu1A-ox-Eu2A] (Fig. 1b), which as

**Table. 1** Crystal data and structure refinement for complexes **1-3**

| Complex | **1** | **2** | **3** |
|---|---|---|---|
| Empirical formula | $C_{42}H_{26}N_4O_{13}Eu_2$ | $C_{42}H_{26}N_4O_{13}Tb_2$ | $C_{42}H_{26}N_4O_{13}Yb_2$ |
| Formula weight | 1098.59 | 1112.51 | 1140.75 |
| Crystal system | Triclinic | Triclinic | Triclinic |
| space group | $P\bar{1}$ | $P\bar{1}$ | $P\bar{1}$ |
| a(Å) | 10.9563(8) | 10.8919(15) | 10.7901(9) |
| b(Å) | 12.8519(10) | 12.8520(17) | 12.8494(10) |
| c(Å) | 14.8421(12) | 14.933(2) | 15.0261(12) |
| α(°) | 70.974(2) | 70.463(3) | 69.5730(10) |
| β(°) | 83.543(2 | 82.650(2) | 81.107(2) |
| γ(°) | 86.737(2) | 85.850(3) | 84.518(2) |
| Volume ($Å^3$) | 1962.7(3) | 1952.8(5) | 1926.9(3) |
| Z | 2 | 2 | 2 |
| Calculated density / g· $cm^{-3}$ | 1.859 | 1.892 | 1.966 |
| Absorption coefficient/ $mm^{-1}$ | 3.240 | 3.667 | 4.899 |
| F(000) | 1072 | 1080 | 1100 |
| Crystal size / $mm^3$ | 0.20x0.15x0.07 | 0.21x0.16x0.10 | 0.22x0.12x0.05 |
| θ range for data collection / (°) | 1.87 to 25.01 | 1.68 to 25.01 | 1.82 to 25.01 |
| Limiting indices | -12≦h≦13;<br>-15≦k≦14;<br>-17≦l≦16 | -12<=h<=12;<br>-15<=k<=11;<br>-17<=l<=17 | -10≦h≦12;<br>-15≦k≦14;<br>-17≦l≦15 |
| Reflections collected/unique | [R(int)= 0.0491]<br>9889 / 6854 | [R(int)= 0.0536]<br>19330 / 6834 | [R(int)= 0.0436]<br>9586 / 6732 |
| Data / restraints / parameters | 6854 / 3 / 556 | 6834 / 15 / 556 | 6732 / 15 / 556 |
| Goodness-of-fit on $F^2$ | 0.995 | 0.822 | 0.913 |
| Final R indices[I>2sigma(I)] | R1 = 0.0554<br>wR2 = 0.1074 | R1 = 0.0570<br>wR2 = 0.0770 | R1 = 0.0478<br>wR2 = 0.0935 |
| R indices(all data) | R1 = 0.0870<br>wR2 = 0.1297 | R1 = 0.1191<br>wR2 = 0.0953 | R1 = 0.0742<br>wR2 = 0.1074 |
| Largest difference peak and hole / e.$Å^{-3}$ | 0.879 and -0.840 | 1.219 and -1.151 | 0.971 and -0.872 |
| CCDC No. | 1040769 | 1040770 | 1040772 |

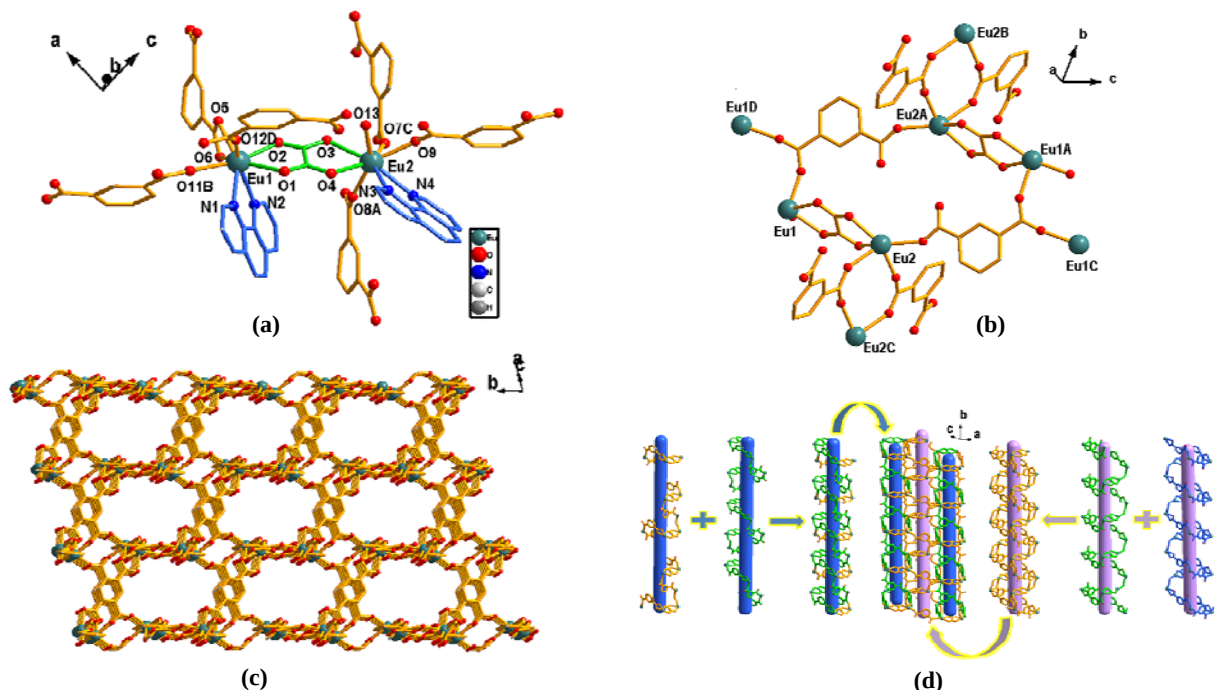


Fig 1. View of the structure of **1**: (a) Coordination environment of the Eu(III) ion. Symmetry codes: A: −1+x, y, z; B: 1+x, y, -1+z; C: 3−x, −y, -1−z D: 2-x, 1-y, -1-z. (b) The centrosymmetric tetradmeric unit. (c) 3D framework. Phen molecules and H atoms are omitted for clarity. (d) The triflexural helix.

secondary building units (SBUs) are assembled into a 3D structure through 1,3-BDC ligands (Fig. 1c). The adjacent two Eu1 ions are interconnected by one $COO^-$ group from 1,3-BDC ligand while adjacent two Eu2 ions are interconnected by two $COO^-$ groups from 1,3-BDC ligand within the 3D structure. The distances of adjacent Eu1 and Eu2 ions, adjacent Eu1 ions, and adjacent Eu2 ions are 6.233(7), 5.575(7), and 5.542(7) Å, respectively. The most fascinating structural feature in **1** is the presence of helix. The helix has a repeating unit consisting of four Eu(II) centers, three 1.3-BDC ligands and one ox ligand with a pitch of 22.804 Å along b axis (Fig. 1d). Eu1 and Eu2 ions are uninodal, and the overall structure of **1** adopts the 3D framework with the topology of $(3^3.4^5.5^6.6)$.

Thermogravimetric analysis (TGA) (Fig. S2) of **1** shows a minor weight loss of approximately 4.10% at 119-264 °C. A major weight loss occurs in the temperature range of 367- 482 °C due to the decomposition of organic ligands. The final residual is $Eu_2O_3$. The total observed weight loss of 67.36% is close to the calculated value of 67.88%. The isostructural frameworks lead to the similar thermal decomposition processes to **1**.

### 3.2 Luminescent properties

The photoluminescence of the ligands and complexes were investigated at room temperature. The ligands are important in determining the emission intensity of the Ln(III) complexes. The emission spectra of the ligands present a broad band centered at 398 nm for 1,3-BDC (λex= 350 nm), at 432 nm with shoulder peak of 458 nm for phen (λex= 350 nm) and for ox (λex= 396 nm) (Fig. 2). Complex **3** presents a broad emission band centered at 452 nm (λex= 350 nm), which are assigned to the typical *π-π transition of ligands (Fig. 2). The red shift (20-54 nm) compared to the ligand emissions is presumably due to the conformational change in ligand upon binding with metal ion (Lifetimes of complex **3** and ligands see in Fig. S3, Table S2). Complexes **1** and **2** emit a bright red and green light in the solid state under UV light, respectively. T.. excitation spectra of **1** and **2** were obtained by monitoring at 613 nm ($^5D_0 \rightarrow {}^7F_2$ for Eu(III)) and 545 nm

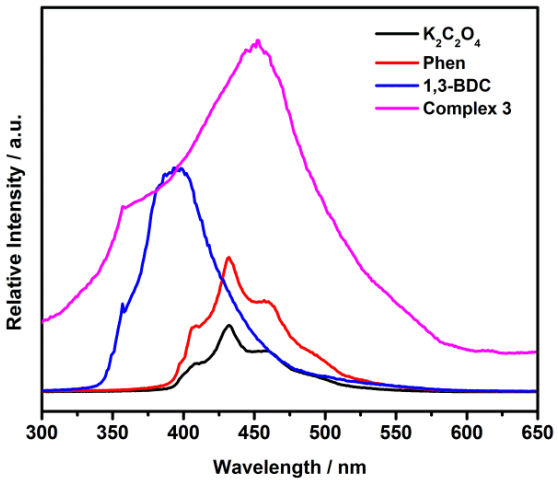


Fig 2. The emission spectra of complex **3** and the free ligands.

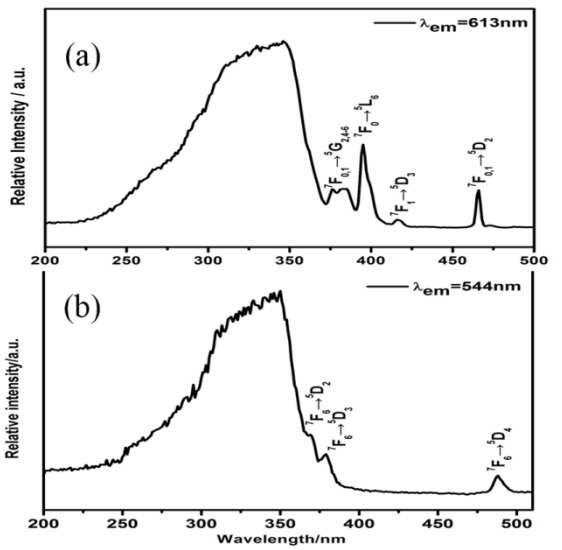


Fig 3. Excitaton spectra of complexes **1** (a) and **2** (b) .

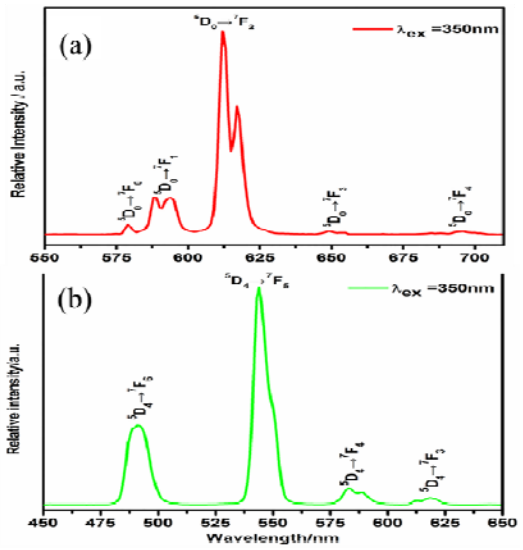


Fig 4. Emission spectra of complexes **1** (a) and **2** (b).

($^5D_4 \rightarrow {}^7F_5$ for Tb(III)), respectively, which consist of a large broad band and several weak narrow bands (Fig. 3). The broad band centered at 350 nm between 220 and 400 nm corresponds to the ligand electronic transitions (π-π* transition) in **1** and **2**. The narrow bands are assigned to the transitions from the $^7F_{0,1}$ ground state to $^5G_{2,4\text{-}6}$ (377-384 nm), $^5L_6$ (395 nm), $^5D_3$ (416 nm) and $^5D_2$ (466 nm) of Eu(III) ion in **1**, and to the transitions from the $^7F_6$ ground state to $^5D_2$ (370 nm), $^5D_3$ (380 nm) and $^5D_4$ (488 nm) of Tb(III) ion in **2**.[11] This indicates that complexes **1** and **2** can be excited both by the ligands and the f–f absorption of Eu(III) and Tb(III). However, the f–f transitions are weaker than the absorption of the organic ligand, which proves that luminescence sensitization via excitation of the ligands is a more efficient pathway than the f–f direct excitation. Under the excitation at the ligand excitation maxima of 350 nm, the emission spectrum of **1** exhibits the characteristic narrow bands arising from the f–f transitions of the Eu(III) (Fig. 4a). The $^5D_0 \rightarrow {}^7F_0$ transition is very weak and is situated at 579 nm. The strong transition of $^5D_0 \rightarrow {}^7F_1$ splits into two peaks at 588 and 594 nm. The emission at 612 nm with a shoulder of 617 nm from the $^5D_0 \rightarrow {}^7F_2$ hypersensitive transition is the strongest. The intensity ratio of 5.49 for $I(^5D_0 \rightarrow {}^7F_2):I(^5D_0 \rightarrow {}^7F_1)$ suggests the chemical environment around Eu(III) ion does not exist in any inversion center.[11] The peaks at 650 nm and 705 nm correspond to the $^5D_0 \rightarrow {}^7F_3$ and $^5D_0 \rightarrow {}^7F_4$ transitions, respectively. Upon excitation at 350 nm, the emission spectrum of **2** consists of four main peaks at 492, 545, 582, and 620 nm, which correspond to the $^5D_4 \rightarrow {}^7F_J$ (J = 6-3) transitions, respectively (Fig. 4b). The emission band at 545 nm ($^5D_4 \rightarrow {}^7F_5$) is obviously stronger than the others and is responsible for the green luminescence under UV irradiation. The luminescent properties of **1** and **2** were also investigated at f–f absorption (395 nm for **1** and 379 nm for **2**) (Fig. S4). The emission intensity of **1** and **2** at f–f absorption is less than that at the ligand excitation maxima, indicating an efficient ligand-to-metal energy transfer process. The ligand broad emission band in **1** and **2** completely disappears, which indicates the ligand as light-harvesting chromophore effectively transfers energy to Eu(III)/Tb(III) ions. Notably, complexes **1** and **2** have high fluorescence quantum yields of 63.21% and 10.13%, respectively. These results clearly indicate that the ligands are excellent antenna chromophores for sensitizing both Tb(III) and Eu(III) ions. The efficiency of the ligands as sensitizer is very high for Eu(III) compared to Tb(III). The excited state $^5D_0$ Eu(III) and $^5D_4$ Tb(III) lifetime values (τ) were measured at room temperature for complexes **1** and **2**, by monitoring within

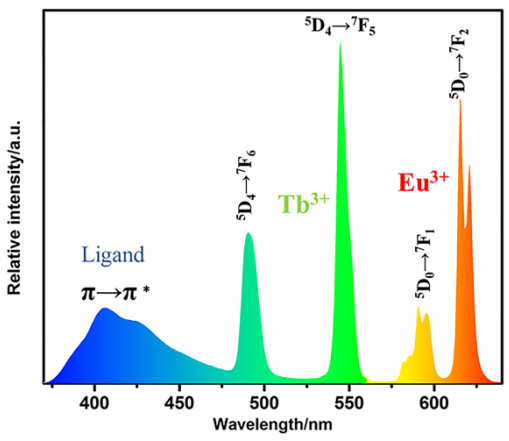


Fig 5. Emission spectrum of the $Yb_{0.73}Tb_{0.25}Eu_{0.02}$ doped complex excited at 355 nm.

**Table. 2** Lifetimes and quantum yields of complexes **1-3** and the doped complex

| Sample | Lifetimes/ms | | Quantum yields, Φ |
|---|---|---|---|
| | $Eu^{3+}$ | $Tb^{3+}$ | |
| Complex **1** | 0.3273 | | 63.21% |
| Complex **2** | | 0.5030 | 10.13% |
| Doped complex | 0.3500 | 0.04182 | 20.4% |

the more intense lines of the $^5D_0 \rightarrow {}^7F_2$ and $^5D_4 \rightarrow {}^7F_5$ transitions, respectively (Table 2, Fig. S3). The decay curve can be well fitted into the bi- exponential function. Lifetime measurements confirm the presence of two local Eu(III)/Tb(III) environments, consistent with the crystal structure.

In order to investigate the multicolor emission, the $Yb_{0.73}Tb_{0.25}Eu_{0.02}$ doped complex was synthesized due to isostructural structures of Yb(III)/Eu(III)/Tb(III) complexes. The emission spectra of the doped complex were recorded under varying excitation wavelengths from 230 to 355 nm. As depicted in Fig. 5, the $Yb_{0.73}Tb_{0.25}Eu_{0.02}$ doped complex shows main narrow emissions at 615 nm for Eu(III) (red) and at 545 nm for Tb(III) (green) as well as a broad emission centered at 405 nm (blue), featured distinctly by f–f transitions from Eu(III) and Tb(III) centers and a ligand centered character from Yb(III)-complex, respectively. It is worth noting that their relative emission (red, green and blue) intensity varies with the excitation wavelengths, leading to multicolor emission from blue, green, yellow to white (Fig. 6) excited at 230, 270, 350 and 355 nm, respectively, due to different energy transfer processes. For example, when excited at 230 nm, the emission with the CIE coordinate of A(0.193,0.207) falls within the blue region. Because the absorbed energy is too low, the ligand fluorescence in the blue region dominates. When excited at 270 nm, the emission peak at 545 nm (Tb(III)) is obviously stronger than the others, leading to the emission with the CIE coordinate of B(0.271, 0.416) falling within the green region. Upon excitation at 350 nm, emission intensity of the red Eu(III) (615 nm) increases and that of green Tb(III) (545 nm) decreases, and thus a yellow emission with CIE coordinates of C(0.373, 0.419) is obtained. Notably, with the excitation wavelength at 355 nm, the emission peaks at the red (615 nm), green (545 nm) and blue (402 nm) light are comparable in intensity, which results in a white-light emission. The chromaticity coordinate at D(0.347, 0.362) is close to the standard white light (0.333, 0.333) according to 1931 CIE coordinate diagram. A col rendering index CRI is 89, a correlated color temperature (CCT) is 4934 K. For high-quality white-light illumination, white-light sources with a CCT between 2500 K and 6500 K and a CRI of above 80 are required.[1d, 12] Most importantly, the quantum yield of white-light emission is up to 20.4%, which is relatively high, compared to that of the many reported MOF-based white light emission.[5j-l] So, the visible emission from blue, green, yellow to white can be achieved with a change of excitation wavelength from 230 to 355 nm. Thus, the doped complex displays ability of tunable luminescence by varying the excitation wavelengths. The present investigation highlights that the tunable white light emission based on LnOFs is highly effective, which is a promising light emissive material. Another important point regards the excitation wavelength of 355 nm that is above ca. 350 nm to facilitate the use of inexpensive excitation sources for instances in the immunoassay applications. It is highly appealing to develop high performance white light emitting materials, which have enormous potential in lighting applications.

In the $Yb_{0.73}Tb_{0.25}Eu_{0.02}$ doped complex, the energy from the ligand as antenna to the central Ln(III) ion results in emissions of the Tb(III) and Eu(III) ions. In fact, the relative excitation

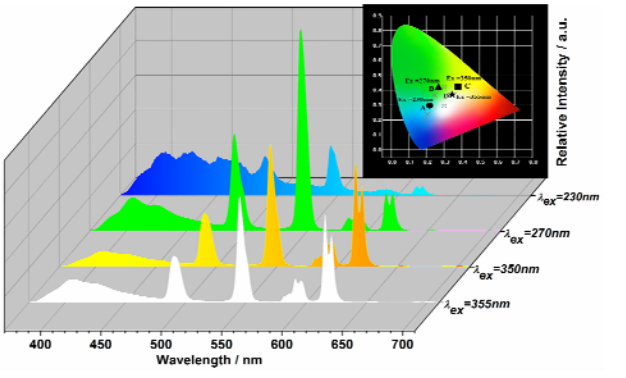


Fig 6. Emission spectra of the $Yb_{0.73}Tb_{0.25}Eu_{0.02}$ doped complex. Inset: The CIE chromaticity diagram.

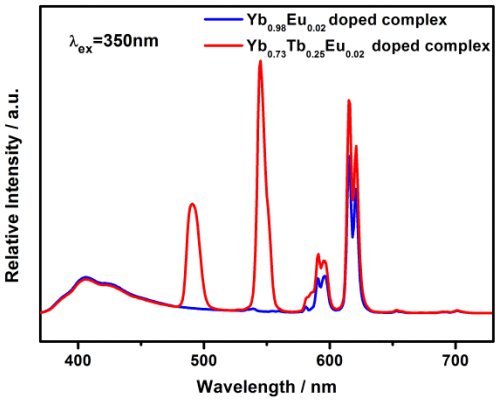


Fig 7. Emission spectra of the $Yb_{0.73}Tb_{0.25}Eu_{0.02}$ and $Yb_{0.98}Eu_{0.02}$ doped complex excited at 350 nm.

energy of Tb(III) ($^5D_4$, 20,400 $cm^{-1}$) is larger than that of Eu(III) ($^5D_0$, 19, 300 $cm^{-1}$),[13] thus indicating that the Tb(III) ion can act as antenna for the photosensitization of Eu(III) ion by the Tb(III) to Eu(III) energy transfer. Therefore, an effective energy transfer from Tb(III) to Eu(III) is expected. To further identify the evidence of the energy transfer from the Tb(III) to Eu(III) ions, the decay curve of the Tb(III) emission was recorded (Fig. S3). The lifetime value of $^5D_4$ Tb(III) in the doped complex is 0.04182 ms, which is less than that in **2**; whereas the lifetime value of $^5D_0$ Eu(III) for the doped complex is 0.3500 ms, which is more than that for **1** , indicating the Tb(III) to Eu(III) energy transfer. Moreover, the addition of Tb(III) to the Eu(III)- doped Yb(III) complex leads to an enhanced luminescent intensity at 617 nm corresponding to the $^5D_0 \rightarrow {}^7F_2$ transition of the Eu(III) ion (Fig. 7), which also supports the Tb(III) to Eu(III) energy transfer. This type of energy transfer has been observed in several Eu(III) and Tb(III) co-complexes.[5e, 6c, 14] According to the equation $\eta_T = 1 - \tau/\tau_0$, where $\eta_T$ is the energy transfer efficiency, and $\tau_0$ and $\tau$ are the lifetimes of a sensitizer in the absence and presence of an activator, respectively, the maximum energy transfer efficiency is 91.68%. It is clear that the Tb(III) center is also acting to sensitize the Eu(III) in the $Yb_{0.98}Eu_{0.02}Tb_{0.8}$ doped complex, effectively enhancing Eu(III) emission.

## Conclusions

1,3- Benzenedicarboxylate - oxalate mixed linkers and 1,10-phenanthroline ancillary ligand were combined successfully to afford novel 3D LnOFs. The frameworks feature helical characteristics with tetranuclear metal ions as SBU nodes. The LnOFs can be successfully used for an efficient tuning of the emission color. A unique blue–green-yellow–white emission for doping low amounts of Eu(III) and Tb(III) into a Yb(III) framework was achieved. Most importantly, a high-efficiency white light emission was obtained. The result gives impetus to the design of novel LnOFs with tunable multicolor luminescence and high-efficiency white light emission.

## Acknowledgements

The authors are grateful to the National Natural Science Foundation of China (21471104) and Scientific Research Base Development Program of the Beijing Municipal Commission of Education.

## Notes and references

Beijing Key Laboratory for Optical Materials and Photonic Devices, Deparment of Chemistry, Capital Normal University, Beijing 100048.
E-mail: xiali@cnu.edu.cn; Fax: +86 10 68902320; Tel: +86 10 68902320.

† Electronic Supplementary Information (ESI) available. CCDC 1040769, 1040770, 1040772. For ESI and crystallographic data in CIF or other electronic format see DOI: 10.1039/b000000x/

1. (a) H. Li, M. Eddaoudi, M. O'Keeffe and O. M. Yaghi, *Nature*, 1999, **402**, 276; (b) J. Lee, O. K. Farha, J. Roberts, K. A. Scheidt, S. T. Nguyen and J. T. Hupp, *Chem. Soc. Rev.*, 2009, **38**, 1450; (c) M. Kurmoo, *Chem. Soc. Rev.*, 2009, **38**, 1353; (d) Y. J. Cui, Y. F. Yue, G. D. Qian and B. L. Chen, *Chem. Rev.*, 2012, **112**, 1126; (e) J. R. Li, R. J. Kuppler and H. C. Zhou, *Chem. Soc. Rev.*, 2009, **38**, 1477.
2. (a) L. Armelao, S. Quici, F. Barigelletti, G. Accorsi, G. Bottaro, M. Cavazzini and E. Tondello, *Coord. Chem. Rev.*, 2010, **254**, 487; (b) M. D. Allendorf, C. A. Bauer, R. K. Bhakta and R. J. T. Houk, *Chem. Soc. Rev.*, 2009, **38**, 1330.
3. (a) P. Horcajada, R. Gref, T. Baati, P. K. Allan, G. Maurin, P. Couvreur, G. Ferey, R. E. Morris and C. Serre, *Chem. Rev.*, 2012, **112**, 1232; (b) L. E. Kreno, K. Leong, O. K. Farha, M. Allendorf, R. P. Van Duyne and J. T. Hupp, *Chem. Rev.*, 2012, **112**, 1105; (c) A. Datta and K. N. Raymond, *Acc. Chem. Res.*, 2009, **42**, 938; (d) P. Caravan, *Chem. Soc. Rev.*, 2006, **35**, 512; (e) M. Bottrill, L. K. Nicholas and N. J. Long, *Chem. Soc. Rev.*, 2006, **35**, 557; (f) F. T. Edelmann, *Chem. Soc. Rev.*, 2009, **38**, 2253; (g) L. Ungur, S. Y. Lin, J. K. Tang and L. F. Chibotaru, *Chem. Soc. Rev.*, 2014, **43**, 6894.
4. (a) M. M. Shang, D. L. Geng, X. J. Kang, D. M. Yang, Y. Zhang and J. Lin, *Inorg. chem.*, 2012, **51**, 11106; (b) F. Wang, X. J. Xue and X. G. Liu, *Angew. Chem. Int. Ed.*, 2008, **47**, 906; (c) H. X. Mai, Y. W. Zhang, L. D. Sun and C. H. Yan, *Chem. Mater.*, 2007, **19**, 4514; (d) A. de Bettencourt-Dias, *Dalton Trans.*, 2007, **22**, 2229; (e) C. H. Huang and T. M. Chen, *Inorg. chem.*, 2011, **50**, 5725; (f) B. H. Kwon, H. S. Jang, H. S. Yoo, S. W. Kim, D. S. Kang, S. Maeng, D. S. Jang, H. Kim and D. Y. Jeon, *J. Mater. Chem.*, 2011, **21**, 12812.
5. (a) D. F. Sava, L. E. S. Rohwer, M. A. Rodriguez and T. M. Nenoff, *J. Am. Chem. Soc.*, 2012, **134**, 3983; (b) A. C. Wibowo, S. A. Vaughn, M. D. Smith and H. C. zur Loye, *Inorg. chem.*, 2010, **49**, 11001; (c) R. S. Liu, V. Drozd, N. Bagkar, C. C. Shen, I. Baginskiy, C. H. Chen and C. H. Tan, *J. Electrochem. Soc.*, 2008, **155**, 71; (d) X. Y. Xu and B. Yan, *Dalton Trans.*, 2015, **44**, 1178; (e) Z. F. Liu, M. F. Wu, S. H. Wang, F. K. Zheng, G. E. Wang, J. Chen, Y. Xiao, A. Q. Wu, G. C. Guo and J. S. Huang, *J. Mater. Chem. C*, 2013, **1**, 4634; (f) Y. H. Zhang, X. Li, S. Song, H. Y. Yang, D. Ma and Y. H. Liu, *Crystengcomm*, 2014, **16**, 8390; (g) S. M. Li, X. J. Zheng, D. Q. Yuan, A. Ablet and L. P. Jin, *Inorg. chem.*, 2012, **51**, 1201; (h) Y. Liu, M. Pan, Q. Y. Yang, L. Fu, K. Li, S. C. Wei and C. Y. Su, *Chem. Mater.*, 2012, **24**, 1954; (i) K. Liu, H. P. You, Y. H. Zheng, G. Jia, Y. J. Huang, M. Yang, Y. H. Song, L. H. Zhang and H. J. Zhang, *Cryst. Growth Des.*, 2010, **10**, 16; (j) D. Ma, X. Li and R. Huo, *J. Mater. Chem. C*, 2014, **2**, 9073; (k) H. B. Zhang, X. C. Shan, L. J. Zhou, P. Lin, R. F. Li, E. Ma, X. G. Guo and S. W. Du, *J. Mater. Chem. C*, 2013, **1**, 888; (l) H. B. Zhang, X. C. Shan, Z. J. Ma, L. J. Zhou, M. J. Zhang, P. Lin, S. M. Hu, E. Ma, R. F. Li and S. W. Du, *J. Mater. Chem. C*, 2014, **2**, 1367; (m) W. Xie, S. R. Zhang, D. Y. Du, J. S. Qin, S. J. Bao, J. Li, Z. M. Su, W. W. He, Q. Fu and Y. Q. Lan, *Inorg. Chem.*, 2015, **54**, 3290; (n) M. Zhu, Z. M. Hao, X. Z. Song, X. Meng, S. N. Zhao, S. Y. Song and H. J. Zhang, *Chem. Commun.*, 2014, **50**, 1912.
6. (a) Y. L. Liu, J. F. Eubank, A. J. Cairns, J. Eckert, V. C. Kravtsov, R. Luebke and M. Eddaoudi, *Angew. Chem. Int. Ed.*, 2007, **46**, 3278; (b) F. Luo, S. R. Batten, Y. X. Che and J. M. Zheng, *Chem. Eur. J.*, 2007, **13**, 4948; (c) H. B. Zhang, L. J. Zhou, J. Wei, Z. H. Li, P. Lin and S. W. Du, *J. Mater. Chem.*, 2012, **22**, 21210; (d) X. J. Gu and D. F. Xue, *Cryst. Growth Des.*, 2006, **6**, 2551; (e) R. L. Chen, X. Y. Chen, S. R. Zheng, J. Fan and W. G. Zhang, *Cryst. Growth Des.*, 2013, **13**, 4428; (f) D. X. Hu, F. Luo, Y. X. Che and J. M. Zheng, *Cryst. Growth Des.*, 2007, **7**, 1733; (g) J. H. He, J. H. Yu, Y. T. Zhang, Q. H. Pan and R. R. Xu, *Inorg. chem.*, 2005, **44**, 9279; (h) M. Du, X. J. Jiang and X. J. Zhao, *Inorg. chem.*, 2007, **46**, 3984; (i) N. L. Rosi, J. Kim, M. Eddaoudi, B. L. Chen, M. O'Keeffe and O. M. Yaghi, *J. Am. Chem. Soc.*, 2005, **127**, 1504.
7. (a) Y. G. Wan, L. P. Zhang, L. P. Jin, S. Gao and S. Z. Lu, *Inorg. chem.*, 2003, **42**, 4985; (b) Y. H. Wan, L. P. Zhang and L. P. Jin, *J. Mol. Struct.*, 2003, **658**, 253; (c) L. P. Zhang, Y. H. Wan and L. P. Jin, *Polyhedron*, 2003, **22**, 981; (d) H. B. Zhang, Y. Peng, X. C. Shan, C. B. Tian, Ping-Lin and S. W. Du, *Inorg. Chem. Commun.*, 2011, **14**, 1165.
8. T. Smith and J. Guild, *Trans. Opt. Soc.*, 1931, **33**, 73.
9. G. M. Sheldrick, SADABS, Program for Empirical Absorption Correction of Area Detector Data, University of Götingen, Götingen, Germany, 1997.
10. (a) G. M. Sheldrick, *SHELXS-97*, Program for Crystal Structure Refinement, University of Göttingen (1997); (b) G. M. Sheldrick, *SHELXL-97*, Program for Crystal Structure Solution, University of Göttingen (1997).
11. (a) C. Ritchie, V. Baslon, E. G. Moore, C. Reber and C. Boskovic, *Inorg. chem.*, 2012, **51**, 1142; (b) S. P. Liu, M. L. Chen, B. C. Chang and K. H. Lii, *Inorg. chem.*, 2013, **52**, 3990.
12. (a) S. V. Eliseeva and J. C. G. Bunzli, *Chem. Soc. Rev.*, 2010, **39**, 189; (b) B. W. D'Andrade and S. R. Forrest, *Adv. Mater.*, 2004, **16**, 1585.

13. (a) C. Zhan, S. Ou, C. Zou, M. Zhao and C. D. Wu, *Anal. Chem.*, 2014, **86**, 6648; (b) N. Chatterton, Y. Bretonniere, J. Pecaut and M. Mazzanti, *Angew. Chem. Int. Ed.*, 2005, **44**, 7595.
14. (a) P. C. R. Soares-Santos, L. Cunha-Silva, F. A. A. Paz, R. A. S. Ferreira, J. Rocha, T. Trindade, L. D. Carlos and H. I. S. Nogueira, *Cryst. Growth Des.*, 2008, **8**, 2505; (b) M. L. Ma, C. Ji and S. Q. Zang, *Dalton Trans.*, 2013, **42**, 10579; (c) D. T. de Lill, A. de Bettencourt-Dias and C. L. Cahill, *Inorg. chem.*, 2007, **46**, 3960; (d) S. Mohapatra, S. Adhikari, H. Riju and T. K. Maji, *Inorg. chem.*, 2012, **51**, 4891; (e) Q. Tang, S. X. Liu, Y. W. Liu, D. F. He, J. Miao, X. Q. Wang, Y. J. Ji and Z. P. Zheng, *Inorg. chem.*, 2014, **53**, 289.

# New lanthanide coordination frameworks constructed from 1,3- benzenedicarboxylate-oxalate mixed linkers and terminal 1,10-phenanthroline: Crystal structure, multicolor luminescence and high-efficiency white light emission

Rui Huo, Xia Li,* and Dou Ma

3D frameworks $[Ln_2(1,3\text{-BDC})_2(phen)_2(ox)(H_2O)]$ (Ln = Eu **1**, Tb **2**, and Yb **3**, 1,3- BDC = 1,3- benzenedicarboxylate, ox = oxalate, and phen = 1,10-phenanthroline) constructed from tetrameric $Ln_4$ as SBUs by 1,3-BDC and ox. The Yb:Tb,Eu doped complex reveals a significant multicolor luminescence. A high-efficiency white light emission was achieved.